Inorg. Chem. **2007**, *46*, 11291–11296

Synthesis of Pendant-Type Anthraquinone-Bridged Cofacial Dinuclear Platinum(II) Complexes and Their Emission Properties

Mitsuya Utsuno, Tomona Yutaka, Masaki Murata, Masato Kurihara,[†] Naoto Tamai,[‡] and Hiroshi Nishihara*

Department of Chemistry, School of Science, The University of Tokyo, Hongo, Bunkyo-ku, Tokyo 113-0033, Japan, Department of Biological Chemistry, Faculty of Science, Yamagata University, 1-4-12 Kojirakawa-machi, Yamagata 990-8560, Japan, Department of Chemistry, Faculty of Science, Kwansei Gakuin University, 2-1 Gakuen, Sanda, Hyogo 669-1337, Japan

Received May 17, 2007

Anthraquinone-bridged mononuclear and dinuclear complexes, [PtCl(AQ-*amide*-tpy)](PF_6) (**1**), [Pt_2Cl_2(AQ-*amide*-tpy_2)]$(PF_6)_2$ (**2**), and [Pt_2Cl_2(AQ-*eth*-tpy_2)]$(PF_6)_2$ (**3**), were synthesized and their photochemical properties were investigated. Amide-bound mononuclear complex **1** exhibited only metal-to-ligand charge transfer (MLCT) absorption and emission, whereas dinuclear complex **2** exhibited a low-energy emission around 700 nm at room temperature. Emission lifetime analysis indicated that this emission was originated from the metal–metal-to-ligand charge transfer (MMLCT) excited state, implying the existence of an intramolecular Pt–Pt interaction at the photoexcited state. **3** with rigid ethynylene linkers showed a low-energy absorption around 520 nm ($\epsilon = \sim$1100 M^{-1} cm^{-1}) in addition to an ^{1}MLCT absorption, which was ascribed to a ^{3}MLCT absorption from the consideration of the Pt–Pt distance on a geometry-optimized structure. The emission of **3** appeared at 600 nm, which is higher in energy compared with the emission of **2**. It is postulated that the restriction of the Pt–Pt distance flexibility in the rigid structure of **3** prevents the significant increase of the Pt–Pt interaction at the excited state.

Introduction

Emissive materials have attracted much recent attention because of their potential to be applied to luminescent probes,[1] dye-amplified solar cells,[2] light-emitting diodes,[3] and so on. In addition to organic materials, transition-metal complexes have been strong candidates for employment in these applications for decades.[4] Platinum(II) complexes with a square-planar d^8 configuration are well-known emissive molecules that, interestingly, can afford various luminescence properties by forming linear dimers or oligomers originating from the interaction between the d_z^2 orbital of central metal ions. Remarkable and tunable luminescent properties of platinum terpyridine complexes, given as $[Pt(tpy)X]^+$, have been reported.[5] Mononuclear $[Pt(tpy)X]^+$ complexes exhibit emissions based on ligand-centered (LC) and metal-to-ligand charge transfer (MLCT) states, and they also show emissions based on the metal−metal-to-ligand charge transfer (MMLCT) excited-state resulting from the intermolecular interaction of platinum centers.[6] The formation of dimeric structures of platinum(II) complexes has been identified by crystal structure analysis, which has shown that the distance between two interacting platinum centers in neighboring molecules is ∼3.3 Å.[6]

* To whom correspondence should be addressed. E-mail: nisihara@chem.s.u-tokyo.ac.jp, Phone: +81-3-5841-4346, Fax: +81-3-5841-8063.
[†] Yamagata University.
[‡] Kwansei Gakuin University.

(1) Cusumanno, M.; Di Pietro, M. L.; Giannetto, A. *Inorg. Chem.* **1999**, *38*, 1754−1758.
(2) (a) Islam, A.; Sugihara, H.; Hara, K.; Singh, L. P.; Katoh, R.; Yanagida, M.; Takahashi, Y.; Murata, S.; Arakawa, H.; Fujihashi, G. *Inorg. Chem.* **2001**, *40*, 5371−5380. (b) McGarrah, J. E.; Kim, Y. J.; Hissler, M.; Eisenberg, R. *Inorg. Chem.* **2001**, *40*, 4510−4511. (c) McGarrah, J. E.; Eisenberg, R. *Inorg. Chem.* **2003**, *42*, 4355−4365.
(3) (a) Adamovich, V.; Brooks, J.; Tamayo, A.; Alexander, A. M.; Djurovich, P. L.; D'Andrade, B. W.; Adachi, C.; Forrest, S. R.; Thompson, M. E. *New. J. Chem.* **2002**, *26*, 1171−1178. (b) Lin, Y. Y.; Chan, S. C.; Chan, M. C. W.; Hou, Y. J.; Zhu, N.; Che, C. M.; Liu, Y.; Wang, Y. *Chem.—Eur. J.* **2003**, *9*, 1263−1272. (c) Lu, W.; Mi, B. X.; Chan, M. C. W.; Hui, Z.; Che, C. M.; Zhu, N.; Lee, S. T. *J. Am. Chem. Soc.* **2004**, *126*, 4958−4971.
(4) (a) Juris, A.; Balzani, V.; Berigelletti, F.; Campagna, S.; Besler, P.; von Zelewsky, A. *Coord. Chem. Rev.* **1988**, *84*, 85−277. (b) Hagfeldt, A.; Grätzel, M. *Acc. Chem. Res.* **2000**, *33*, 269−277. (c) Grushin, V. V.; Herron, N.; LeCloux, D. D.; Marshall, W. J.; Petrov, V.; A.; Wang, Y. *Chem. Commun.* **2001**, 1494−1495.
(5) Jenette, K. W.; Gill, J. T.; Sadownick, J. A.; Lippard, S. J. *J. Am. Chem. Soc.* **1976**, *98*, 6159−6168.
(6) Bailey, J. A.; Hill, M. G.; Marsh, R. E.; Miskowski, V. M.; Schaefer, W. P.; Gray, H. B. *Inorg. Chem.* **1995**, *34*, 4591−4599.

10.1021/ic700953k CCC: $37.00
Published on Web 11/29/2007

Chart 1. Anthraquinone-Bridged Platinum Complexes

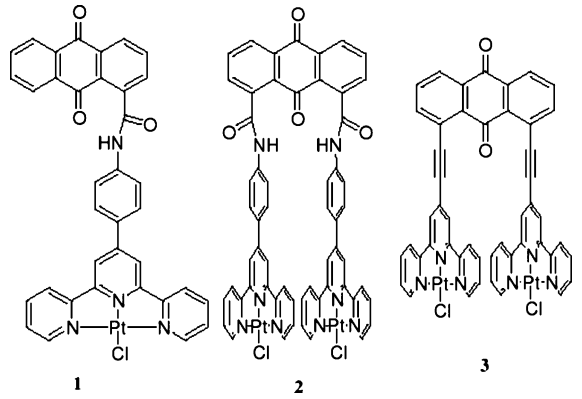

Luminescence of dinuclear platinum complexes with an electronic interaction between platinum d_z^2 orbitals has been investigated for $[Pt_2(pop)_4]^{4-}$ (pop = $H_2P_2O_5^{2-}$, diphosphonate) for three decades.[7] However, it is only recently that luminescence properties of platinum dinuclear complexes with polypyridine ligands have been reported; one example involves two platinum bipyridine complex moieties bridged by pyridyl thiolate,[8] and the other is made of two Pt(tpy)X (tpy = terpyridine) units that are bound through the X position.[9] We describe here new pendant-type dinuclear complexes in which two platinum terpyridine complex units are bound at the 4′ position of terpyridine and anthraquinone introduced as a spacer (Chart 1). These dinuclear complexes were designed to make the Pt−Pt distance short enough so that the complexes could be located side-by-side, on the basis of steric requirements. As the linking moiety, a flexible amide bond and a rigid ethynylene bond were employed so that the effects of the distance between the two platinum ions and the rigidity of the structure on the photochemical properties were determined. The synthesis, characterization, and luminescence properties, including analysis of the time-transient spectra of the complexes, are described in this article.

Experimental Section

Materials. Anthraquinone-1-carboxylic acid,[10] anthraquinone-1,8-dicarboxylic acid,[11] 1,8-diaminoanthraquinone,[12] 4′-(4-aminophenyl)-2,2′;6′,2″-terpyridine (anilino-tpy),[13] 4′-ethynyl-2,2′;6′,2″-terpyridine,[14] $Pd(PPh_3)_4$,[15] and dichlorobis(dimethyl sulfoxide)-platinum(II) ($PtCl_2[dmso]_2$)[16] were prepared as previously reported. Anthraquinone-1-carbonyl chloride,[17] anthraquinone-1,8-dicarbonyl chloride,[17] and 1,8-dibromoanthraquinone[18] were synthesized as previously reported from anthraquinone-1-caroboxylic acid, anthraquinone1,8-dicarboxylic acid, and 1,8-diaminoanthraquinone, respectively. For UV−vis absorption and emission spectroscopy, *N*,*N*-dimethylformamide, acetonitrile, ethanol, and methanol (spectroscopic grade; Kanto Chemicals, Tokyo) were used as received. Other reagents were obtained from commercial sources and used as received.

Apparatus. UV−vis spectra were measured with Jasco V-570 and Hewlett-Packard 8453 UV−vis spectrometers, IR spectra with a Jasco FT/IR-620v spectrometer, ^{1}H NMR spectra with JEOL EX270 (270 MHz) and Bruker DRX 500 (500 MHz) spectrometers, FAB MS spectra with a JEOL JMS-SX102 spectrometer, and MALDI-TOF MS spectra with SHIMADZU/KRATOS Kompact SEQ and SHIMADZU/KRATOS AXIMA-CFR time-of-flight mass spectrometers.

Anthraquinone-1-carboxylic Acid (4-[2,2′;6′,2″]Terpyridine-4′-yl-phenyl)amide (AQ-*amide*-tpy). To a solution of anilino-tpy (0.25 g, 0.78 mmol) dissolved in a minimum volume of chloroform was added triethylamine (1 mL) followed by anthraquinone-1-carbonyl chloride (0.21 g, 0.78 mmol). The mixture was refluxed for 3 h to give a brown suspension. After the mixture was cooled to room temperature, the white precipitate was filtered, washed with chloroform and ether, and dried in vacuo. The white solid was obtained in a yield of 0.070 g (16%). ^{1}H NMR (DMSO-d_6): δ 10.6 (s, 1H); 8.77 (t, J = 8.1 Hz, 3H); 8.68 (d, J = 7.8 Hz, 2H); 8.36 (dd, J = 7.6, 1.6 Hz, 2H); 8.24 (m, 1H); 8.17 (m, 1H); 8.03 (m, 4H); 7.96 (d, J = 7.6 Hz, 6H); 7.54 (t, J = 5.7 Hz, 2H). Anal. Calcd for $C_{36}H_{22}N_4O_3$: C, 77.41; H, 3.97, N, 10.03. Found: C, 77.22; H, 4.07; N, 9.97.

Anthraquinone-1,8-dicarboxylic Acid Bis[(4-[2,2′;6′,2″]terpyridine-4′-yl-phenyl)amide] (AQ-*amide*-tpy$_2$). AQ-*amide*-tpy$_2$ was prepared from anthraquinone-1,8-dicarbonyl chloride (0.13 g, 0.38 mmol) and anilino-tpy (0.25 g, 0.77 mmol) in a manner similar to that used for the preparation of AQ-*amide*-tpy. A yellow solid was obtained in a yield of 0.13 g (36%). ^{1}H NMR (DMSO-d_6): δ 10.1 (s, 2H); 8.43 (d, J = 4.3 Hz, 4H); 8.34 (d, J = 7.6 Hz, 2H); 8.28 (t, J = 7.0 Hz, 8H); 7.99 (m, 4H); 7.83 (t, J = 7.8 Hz, 4H); 7.59 (s, 8H); 7.26 (t, J = 4.6 Hz, 4H). Anal. Calcd for $C_{58}H_{36}N_8O_4 \cdot 9/4C_2H_6SO$: C, 69.20; H, 4.60, N, 10.33. Found: C, 69.51; H, 4.58; N, 10.21. FAB-MS (m/z): 909.4 ($C_{58}H_{36}N_8O_4^+$ requires 908.96).

1,8-Bis[2,2′;6′,2″]terpyridine-4′-yl-ethynyl-anthraquinone (AQ-*eth*-tpy$_2$). A solution of 1,8-dibromoanthraquinone (0.37 g, 1.00 mmol), 4′-ethynyl-2,2′;6′,2″-terpyridine (0.52 g, 2.0 mmol), $Pd(PPh_3)_4$ (32 mg, 0.028 mmol), and copper(I) iodide (4.5 mg, 0.024 mmol) in triethylamine (60 mL) was refluxed for 16 h under N_2. After complete consumption of the starting materials (confirmed by TLC), the mixture was cooled to room temperature, and the solvent was evaporated to give a green residue. The residue was dissolved in chloroform, and the solution was washed with water. The organic layer was separated and dried with Na_2SO_4. After filtration and evaporation of the solvent, the crude product was chromatographed on an alumina column (activity III). After the resulting pale-yellow fraction was completely eluted using hexane−

(7) Roundhill, D. M.; Gray, H. B.; Che, C.-M. *Acc. Chem. Res.* **1989**, *22*, 55−61.
(8) Kato, M.; Omura, A.; Toshikawa, A.; Kishi, S.; Sugimoto, Y. *Angew. Chem., Int. Ed.* **2002**, *41*, 3183−3185.
(9) (a) Yip, H.-K.; Che, C.-M.; Zhou, Z.-Y.; Mak, T. C. W. *J. Chem. Soc., Chem. Commun.* **1992**, 1369−1371. (b) Bailey, J. A.; Miskowski, V. M.; Gray, H. B. *Inorg. Chem.* **1993**, *32*, 369−370.
(10) Golden, R.; Stock, L. M. *J. Am. Chem. Soc.* **1972**, *94*, 3080−3088.
(11) Rogers, M. E.; Averill, B. A. *J. Org. Chem.* **1986**, *51*, 3308−3314.
(12) Perry, P. J.; Reszka, A. P.; Wood, A. A.; Read, M. A.; Gowan, S. M.; Dosanjh, H. S.; Tremt, J. O.; Jenkins, T. C.; Kelland, L. R.; Neidle, S. *J. Med. Chem.* **1998**, *41*, 4873−4884.
(13) Storrier, G. D.; Colbran, S. B.; Craig, D. C. *J. Chem. Soc., Dalton. Trans.* **1997**, 3011−3028.
(14) Grosshenny, V.; Romero, F. R.; Ziesell, R. *J. Org. Chem.* **1997**, *62*, 1491−1500.
(15) Dangles, O.; Guibe, F.; Balavoine, G. *J. Org. Chem.* **1987**, *52*, 4984−4993.
(16) Price, J. H.; Williamson, A. N.; Schramin, R. F.; Wayland, B. B. *Inorg. Chem.* **1972**, *11*, 1280−1284.
(17) (a) Leon, J. W.; Whitten, D. G. *J. Am. Chem. Soc.* **1995**, *117*, 2226−2235. (b) Waldman, H.; Stengel, R. *Chem. Ber.* **1950**, *83*, 167−170. (c) Beckett, A. H.; Walker, J. *Tetrahedron* **1963**, *19*, 545−556.
(18) Doyle, M. P.; Siegfried, B.; Dellaria, J. F., Jr. *J. Org. Chem.* **1977**, *42*, 2426−2431.

ethyl acetate (1:1 v/v) as an eluent, further elution with dichloromethane gave a yellow-brown fraction. This fraction was collected, the solvent was evaporated, and the residue was recrystallized from dichloromethane−hexane to afford a yellow solid in a yield of 0.37 g (51%). ^{1}H NMR (500 MHz, $CDCl_3$): δ 8.65 (s, 4H); 8.39 (d, J = 4.8 Hz, 4H); 8.36 (d, J = 7.9 Hz, 2H); 8.31 (d, J = 7.9 Hz, 4H); 8.05 (dd, J = 4.8, 1.1 Hz, 2H); 7.80 (t, J = 4.8 Hz, 2H); 7.71 (td, J = 7.9, 1.3 Hz, 4H); 7.10 (ddd, J = 7.9, 4.8, 1.2 Hz, 4H). IR (KBr, cm^{-1}) 2209 (w), 1675, 1636. Anal. Calcd for $C_{48}H_{26}N_6O_2\cdot H_2O$: C, 78.25; H, 3.83, N, 11.41. Found: C, 78.25; H, 3.80; N, 11.08. MALDI-TOF MS: 719.07 ($C_{48}H_{26}N_6O_2$ + 1H requires 719.21).

General Procedure for Preparation of the Platinum Complexes. $PtCl_2(dmso)_2$ was dissolved in DMSO, to which $AgCF_3SO_3$ (1 equiv) in DMSO was added. After stirring for 20 h, the mixture was filtered through Celite to remove the gray AgCl precipitate. The pale-yellow solution was heated at 100 °C, and ligand (1 equiv for a mononuclear complex and 0.5 equiv for a dinuclear complex) was added. The color changed, and the solution was heated for 2 h, followed by cooling to room temperature and filtration. The precipitate formed by the addition of excess NH_4PF_6 in water was filtered off and recrystallized from acetonitrile−ether.

[PtCl(AQ-*amide*-tpy)](PF$_6$) (1). Complex **1** was obtained as an orange-yellow solid from $PtCl_2(dmso)_2$ (0.048 g, 0.11 mmol), $AgCF_3SO_3$ (0.029 g, 0.11 mmol), and AQ-*amide*-tpy (0.064 g, 0.11 mmol) in a yield of 0.089 g (85%). ^{1}H NMR(DMSO-d_6): δ 10.7 (s, 1H); 8.96 (s, 2H); 8.90 (d, J = 4.9 Hz, 2H); 8.83 (d, J = 7.6 Hz, 2H); 8.53 (t, J = 7.8 Hz, 2H); 8.34 (d, J = 7.6 Hz, 2H); 8.26 (dd, J = 5.4, 2.4 Hz, 4H); 8.13 (dd, J = 8.1, 2.7 Hz, 1H); 8.04 (t, J = 7.3 Hz, 2H); 7.95 (m, 5H). Anal. Calcd for $C_{36}H_{22}N_4O_3ClPF_6Pt\cdot H_2O$: C, 45.41; H, 2.54, N, 5.88. Found: C, 45.68; H, 2.87; N, 6.12. MALDI-TOF MS: 787.8 ($C_{36}H_{22}N_4O_3ClPt$ requires 789.12).

[Pt$_2$Cl$_2$(AQ-*amide*-tpy$_2$)](PF$_6$)$_2$ (2). Complex **2** was obtained as a red solid from $PtCl_2(dmso)_2$ (0.24 g, 0.49 mmol), $AgCF_3SO_3$ (0.12 g, 0.49 mmol), and AQ-*amide*-tpy$_2$ (0.22 g, 0.24 mmol), in a yield of 0.31 g (76%). Anal. Calcd for $C_{58}H_{36}N_8O_4Cl_2P_2F_{12}Pt_2\cdot H_2O$: C, 41.52; H, 2.28; N, 6.68. Found: C, 41.70; H, 2.72; N, 6.38. MALDI-TOF MS: 1370.25 ($C_{58}H_{36}N_8O_4Cl_2P_2F_{12}Pt_2$ + 1H requires 1370.16).

[Pt$_2$Cl$_2$(AQ-*eth*-tpy$_2$)](PF$_6$)$_2$ (3). Complex **3** was obtained as a dark-brown solid from $PtCl_2(dmso)_2$ (0.12 g, 0.28 mmol), $AgCF_3SO_3$ (0.071 g, 0.27 mmol), and AQ-*eth*-tpy$_2$ (0.10 g, 0.14 mmol), in a yield of 0.11 g (52%). IR (KBr, cm^{-1}) 2105, 1673, 842. Anal. Calcd for $C_{48}H_{26}N_6O_2Cl_2P_2F_{12}Pt_2$: C, 39.23; H, 1.78; N, 5.72. Found: C, 39.14; H, 2.06; N, 5.52. MALDI-TOF MS: 1178.97 ($C_{48}H_{26}N_6O_2Cl_2P_2F_{12}Pt_2$ requires 1179.08).

Time-Resolved Fluorescence Spectroscopy. Luminescence dynamics were measured by a picosecond single-photon timing system equipped with a microchannel-plate photomultiplier (Hamamatsu R3809U; Hamamatsu, Hamamatsu City, Japan). The samples were excited by a second harmonic (415 nm or 420 nm) of a femtosecond titanium/sapphire laser (Tsunami and Millennia Vs; Spectra Physics, Mountain View, CA), for which the repetition rate was reduced to 4 MHz by a pulse picker (Model 25D and 305; Conoptics, Danbury, CT). The samples were measured in ca. 10 μM acetonitrile solutions.

Calculation of Molecular Structures. Molecular structures were calculated by DFT employing the three-parametrized Becke−Lee−Yang−Parr (B3LYP) hybrid functional. As a basis set, 6-31G* was employed for carbon, hydrogen, nitrogen, and oxygen, and LanL2DZ was employed for platinum. Calculations were carried out with *Gaussian 03W* software.

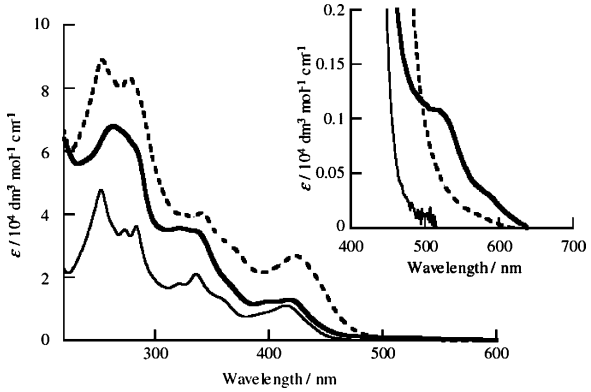

Figure 1. UV−vis absorption spectra of **1** (solid line), **2** (dashed line), and **3** (bold line) in acetonitrile.

Results and Discussion

Absorption Spectroscopy. UV−vis absorption spectra of complexes in acetonitrile are shown in Figure 1 and the data are summarized in Table 1. All of the complexes have an intense absorption band below 300 nm ascribed to the $\pi-\pi^*$ transition of their ligands. Other absorption bands were observed around 420 nm, and were assignable to metal-to-ligand charge transfer (MLCT) bands.[20] In the case of amide-bound complexes, the molar distinction coefficient, ϵ, is 1.1 × 10^4 M^{-1} cm^{-1} for mononuclear complex **1**, and 2.6 × 10^4 M^{-1} cm^{-1} for dinuclear complex **2**, indicating that ϵ is 1.3 × 10^4 M^{-1} cm^{-1} per one platinum complex unit, which is much larger than that of platinum complexes with a nonsubstituted terpyridine ligand ($\epsilon = \sim 5 \times 10^3$ M^{-1}cm^{-1}).[20]

On the other hand, in the case of ethynylene-bound dinuclear complex **3**, ϵ of the MLCT band was 1.3 × 10^4 M^{-1} cm^{-1} (6.5 × 10^3 M^{-1} cm^{-1} per one complex unit), which is similar to that for platinum complexes of nonsubstituted terpyridine. A weak absorption band with $\epsilon = \sim 1000$ M^{-1} cm^{-1} was observed as a shoulder of the MLCT band around 520 nm. This band was not observed in the amide-bonded complexes, **1** and **2**. There are two possibilities in regard to the origin of this low-energy absorption band; one is an MMLCT band originated from intramolecular Pt−Pt interaction as reported by Gray et al. for $[Pt_2(tpy)_2(\mu\text{-Gua})]^{3-}$ (μ-Gua = μ-guanidine) (λ_{max} = 483 nm, ϵ = 2700 M^{-1} cm^{-1}),[9a] $[Pt(tpy)]_2(\mu\text{-pz})$ (pz = pylazole) (λ_{max} = 430 nm, ϵ = 2520 M^{-1} cm^{-1}),[9b] and $[Pt_2(tpy)_2(\mu\text{-dpf})]^{3-}$ (μ-dpf = μ-diphanylformamide) (λ_{max} = 490 nm, ϵ = 3390 M^{-1} cm^{-1}),[9b] and the other is a ^{3}MLCT transition as reported for $[Pt(^tBu_3tpy)Cl]^+$ (λ_{max} = 465 nm, ϵ = 57 M^{-1} cm^{-1}).[21] The intramolecular tpy plane-to-tpy plane distance in ligand **AQ-*eth*-tpy$_2$** estimated from DFT calculation was 4.3 Å, and the intramolecular Pt− Pt distance in **3** was ∼11 Å. Finding the longer distance between two platinum atoms in the complex than the tpy−tpy distance in the ligand can be ascribed to intramolecular electronic repulsion between

(19) Aldridge, T. K.; Stacey, E. M.; McMillin, D. R. *Inorg. Chim. Acta* **1998**, *273*, 346−353.
(20) McMillin, D. R.; Moore, J. J. *Coord. Chem. Rev.* **2002**, *229*, 113−121.
(21) Lai, S.-W.; Chan, M. C. W.; Cheung, K.-K.; Che, C.-M. *Inorg. Chem.* **1999**, *38*, 4262−4267.

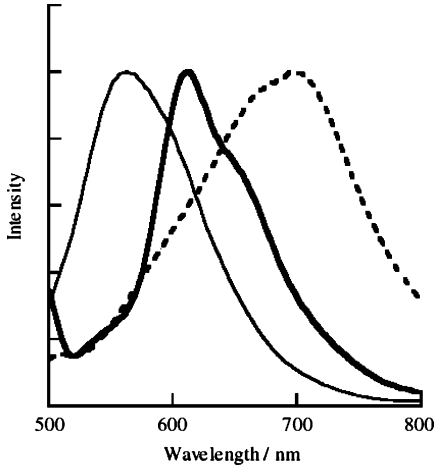

Figure 2. Normalized emission spectra of **1** (solid line), **2** (dashed line), and **3** (bold line) in acetonitrile at 298 K.

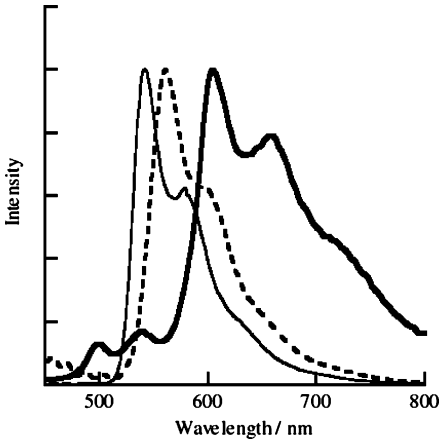

Figure 3. Normalized emission spectra of **1** (solid line), **2** (dashed line), and **3** (bold line) in EMD glass (EtOH/MeOH/DMF = 5:5:1) at 77 K.

cationic platinum centers and that between anionic chloride ligands. The Pt−Pt distance is much longer that for the complexes showing an MMLCT band (the intramolecular Pt−Pt distance is 3.08 Å for $[Pt_2(tpy)_2(\mu\text{-Gua})]^{3-}$ and 3.05 Å for $[Pt_2(tpy)_2(\mu\text{-dpf})]^{3-}$). Thus, we postulate that the 520 nm band is assignable to a ^{3}MLCT transition. The finding that the ^{3}MLCT absorption of **3** had a lower energy and higher intensity compared with that of $[Pt(^tBu_3tpy)Cl]^+$ would be ascribable to the extended π-conjugation in **3**.

Emission Spectroscopy. Figures 2 and 3 show emission spectra of **1**, **2**, and **3** at room temperature at a concentration of ca. 10 μM, which is low enough to be able to neglect the effect of the aggregation of platinum complexes, in an acetonitrile solution and at 77 K in EMD (ethanol/methanol/DMF = 5:5:1) glass, respectively, at an excitation wavelength of the MLCT absorption band. These spectral data are also summarized in Table 2. **1** irradiated by 410 nm light exhibits an emission peak at 550 nm, which is similar to the peaks for previously reported platinum complexes,[20] and was assignable to an emission from the ^{3}MLCT excited state. When **1** was irradiated by UV light (325 nm) to excite an intraligand transition, the same emission spectrum was obtained. This indicates that the ^{3}LC excited-state is inactivated thermally or an energy transfer from ^{3}LC to ^{3}MLCT occurs in fluid solution. Upon excitation at 410 nm at 77 K, an emission peak was observed at 550 nm as well as at room temperature, whereas the intensity was more than 10 times stronger than that at room temperature. Upon excitation by 325 nm light, emission from $\pi-\pi^*$ of the terpyridine moiety was observed at 450−500 nm.

Table 1. UV−vis Absorption Spectral Data of Pt-Complexes in Acetonitrile

complex	λ_{max} / nm (ϵ/M^{-1} cm^{-1})
1	252(47 600), 273(35 100), 283(36 200), 336(21 000), 414(11 000)
2	254(88 900), 277(83 400), 341(40 600), 423(26 800)
3	213(67 100), 263(67 900), 321(35 600), 420(13 000), 518(sh, 1100)

Table 2. Emission Spectral Data of Platinum Complexes in Acetonitrile Solution or EMD Glass

complex	T (K)	solvent	λ_{max} (nm)
1	298	acetonitrile	564
	77	EMD glass	543
2	298	acetonitrile	695
	77	EMD glass	561
3	298	acetonitrile	608
	77	EMD glass	610, 660

In the emission spectrum of **2** on excitation of MLCT by 430 nm light at room temperature, a broad band centered at 700 nm was observed. On the other hand, at 77 K, an emission peak was observed at 560 nm, which was attributed to the ^{3}MLCT emission. Compared to **1**, the MLCT emission was shifted to a longer wavelength region by 10 nm. Considering that the absorption band was also red-shifted, it is supposed that the energy level of MLCT was lowered. The emission at room temperature appeared in an extraordinarily lower-energy region compared to the MLCT emission of the common platinum complexes, suggesting that the emission can be ascribed to the MMLCT emission.

3 exhibited an emission at 600 nm when the MLCT band was irradiated by 420 nm light at room temperature. The emission peak was red-shifted by ca. 50 nm compared with that of **2**, indicating a large Stokes shift. At 77 K, the shape of the emission peaks was similar to that at room temperature, but their intensity was stronger than that at room temperature and approximately 40% of that of **2** at 77 K. The emission of **3** in the region of 650−700 nm was more clearly observed compared with **1** and **2**. This emission is thought to have originated from MMLCT because it was not observed in common mononuclear platinum complexes[5,19,20] and because it was much weaker in other dinuclear complexes.[9]

The concentration dependences of emission spectra for **1**−**3** in EMD glass at 77 K are shown in Figures 4−6. **1** did not show any large spectral change by increasing the concentration to 0.1 mM. This is in contrast to the emission results for $[Pt(tpy)Cl]^+$ at 700 nm, which was assigned to MMLCT; these emissions obviously appeared when the concentration was ca. 0.1 mM.[6] In contrast, a strong dependency of the spectra on the concentration of **2** was observed. The emission around 700 nm was obviously increased above 0.07 mM, and the emission at 550 nm was the most intense at 0.1 mM. The emission around 700 nm was attributed to MMLCT caused by intermolecular Pt−Pt

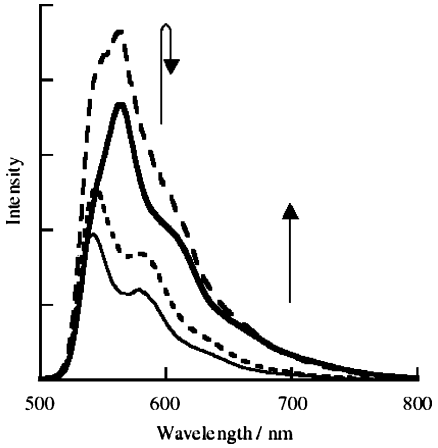

Figure 4. Concentration dependence of the emission spectra of **1** in EMD glass at 77 K. The concentrations of **1** were 0.012 (solid line), 0.027 (dotted line), 0.060 (dashed line), and 0.133 mM (bold line).

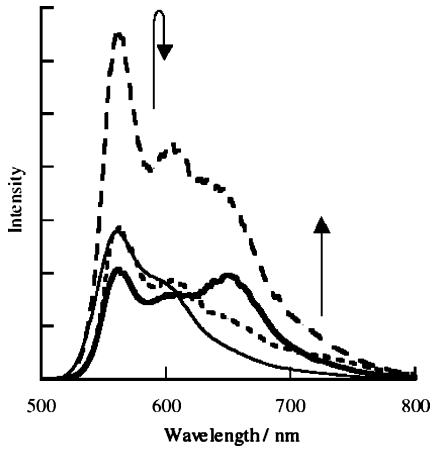

Figure 5. Concentration dependence of the emission spectra of **2** in EMD glass at 77 K. The concentrations of **2** were 0.013 (solid line), 0.029 (dotted line), 0.071 (dashed line), and 0.143 mM (bold line).

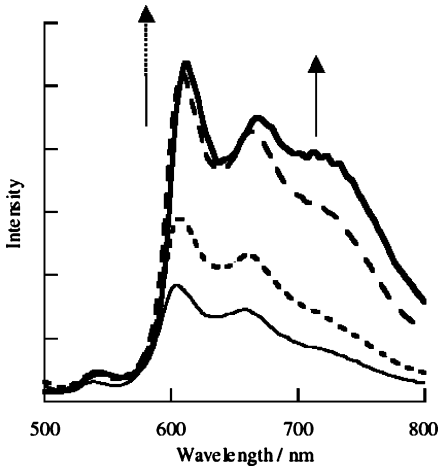

Figure 6. Concentration dependence of the emission spectra of **3** in EMD glass at 77 K. The concentrations of **3** were 0.011 (solid line), 0.021 (dotted line), 0.053 (dashed line), and 0.105 mM (bold line).

interaction, judging from the concentration dependence, suggesting that platinum−terpyridine complex units of two molecules are easier to get close than the mononuclear complex, **1**. This tendency might be caused by the steric interaction between two complex units in a molecule. However, the electronic interaction between the two complex units in **2** is not strong enough to exhibit a characteristic band in both absorption and emission spectra in dilute solution. This is supposed to be due to the flexibility around the amide bond. The concentration dependency of the emission spectra of **3** shows behavior distinct from those of **1** and **2**. The spectral change was less obvious compared with that of **2** up to 0.1 mM. Emissions around 700 nm were already observed in a dilute solution (0.1 M), but their intensity increased with concentration, indicating that the intermolecular Pt−Pt interaction appeared at higher concentrations.

Table 3. Results of Time-Transient Luminescence Spectroscopy in Acetonitrile on 420 nm Light Irradiation

complex	λ_{em} (nm)	τ (ns, amplitude)		
1	550	0.021 (0.985),	0.212 (0.013),	5.72 (0.002)
	650	0.044 (0.939),	0.320 (0.055),	5.78 (0.005)
2	550	0.029 (0.985),	0.430 (0.013),	9.94 (0.002)
	650	0.083 (0.950),	1.210 (0.032),	14.5 (0.017)
3	500	0.0022 (0.999),	2.93 (0.001)	
	600	0.042 (0.765),	0.329 (0.199),	2.72 (0.036)
	650	0.034 (0.778),	0.317 (0.186),	2.10 (0.036)

Emission Lifetime. The emission lifetime was measured by time-resolved fluorescence spectroscopy on excitation with 420 nm light at room temperature in acetonitrile solution of ca.10 μM, at which the aggregation of complexes should not occur. An example of emission decay curves thus obtained is shown in Figure 7. Because the decay behaviors cannot be simply analyzed with a single-exponential curve, a three-component analysis of emission decay curves at a given wavelength was carried out, and the results of the lifetimes and the amplitudes of the components are summarized in Table 3. We first compare the results between monomer **1** and dimer **2**. No significant difference was observed in the emission decay curves between **1** and **2** at 550 nm emission, whereas the emission at 650 nm of **2** comprised longer lifetime components than **1**. The longest component of **1** was 5.8 ns, but that of **2** was 15 ns with larger amplitude, indicating that the emission at 550 nm results from similar excited states, that is, MLCT. In contrast, the 650 nm emission of **2** clearly has excited species different from those of MLCT, and thus should correspond to MMLCT, as mentioned above. Because the concentration is low enough to prevent intermolecular interaction, we identify the long-lifetime component as MMLCT caused by intramolecular Pt−Pt interactions. This existence of MMLCT by the intramolecular Pt−Pt interaction in **2** is contradictory to the results of the UV−vis absorption spectrum, as described above. Two possibilities can be considered as to why MMLCT absorption was not observed in the absorption spectrum of **2**. The first is that the MMLCT absorption band was hidden beyond the MLCT band because the MLCT absorption was extremely intense ($\epsilon_{max} = 2.5 \times 10^5$ $M^{-1}cm^{-1}$), and the second is that overlapping of the platinum d_z^2 orbital hardly occurs at the ground state because of the existence of two conformers, depending on how the amide linkages are placed relative to each other, whereas Pt−Pt interactions can be observed at the MLCT excited-state because a shorter-distance, face-to-face structure was superior between two conformers.

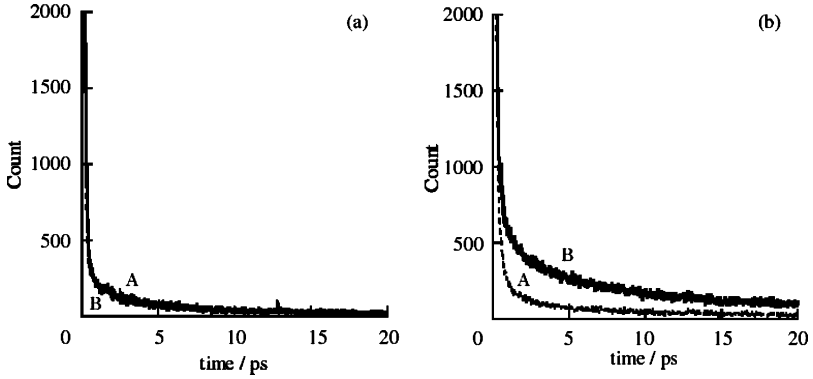

Figure 7. Emission decay spectra of **1** (line A) and **2** (line B). The monitoring wavelength was 550 nm (a) and 650 nm (b).

As for **3**, a component with a considerably short lifetime (2 ps) accounted for the greater part of the emissions at 500 nm, and 300 ps and 2 ns components were exhibited with larger amplitudes in emissions at both 600 and 650 nm than those at 500 nm. Taking into account the excitation spectra shown in Figures S3−5 (Suporting Information), the emission at 500 nm was assignable to a ^{1}MLCT emission. In addition, it is indicated that a 300 ps lifetime can be assigned to ^{3}MLCT, and the 2 ns component is assigned to ^{3}MMLCT. We postulate that the restriction of the Pt−Pt distance flexibility in the more-rigid structure of **3** compared with that of **2** prevents the significant increase of the Pt−Pt interaction at the excited state. Most of the lifetime components of **3** were shorter than those of **2**. It is also likely that the π-conjugated system is expanded via a triple bond, so that quenching of the photoexcited state by energy transfer from the platinum center to the anthraquinone moiety may proceed more efficiently in **3** than in **2**.

Conclusion

New pendant-type dinuclear complexes in which two platinum terpyridine complex units were bridged with an anthraquinone moiety were synthesized. In the case of the amide-bound dinuclear complex, **2**, the intramolecular interaction between two platinum cations was scarcely observed at the ground state, but it existed at the excited state. In contrast, in the triple-bonded dinuclear complex, **3**, intramolecular interaction at the excited-state was weaker than that in complex **2**, preventing a Pt−Pt interaction because of the rigidity of the linkage moiety.

Acknowledgment. This work was supported by Grants-in-Aid for Scientific Research (Grants 16047204 (area 434) and 17205007) and by CREST, JST, Japan.

Supporting Information Available: Structures of ligand AQ-*eth*-tpy$_2$ and **3** calculated with the DFT(B3LYP) method and excitation spectra of **1**−**3** at 298 and 77 K. This material is available free of charge via the Internet at http://pubs.acs.org.

IC700953K